Chemical Engineering Journal 96 (2003) 145–155

Chemical Engineering Journal

www.elsevier.com/locate/cej

Local air ratio measured by zirconia cell in a circulating fluidised bed furnace

Fredrik Niklasson*, Filip Johnsson, Bo Leckner

Department of Energy Conversion, Chalmers University of Technology, 412 96 Göteborg, Sweden

Abstract

This work concerns the local air ratio in a circulating fluidised bed (CFB) furnace, estimated by fluctuating signals from zirconia cell probes and compared to simultaneous analysis of concentrations of extracted gas samples. The time fraction during which the fluctuating zirconia cell signal shows oxidising gas conditions is strongly correlated to the local air ratio of the gas. This correlation is characterised by two parameters that depend on the fuel properties and the position in the furnace. When the two parameters are determined, the fluctuating signals from zirconia cell sensors can be used to obtain the air ratio at different heights in the furnace. This provides a cheap and robust technique for on-line monitoring of the gas conditions in the furnace when, for example, optimising the operation of a CFB boiler to reduce nitrous oxide emissions. The method is limited to the freeboard, because the vivid fluctuations of gas concentrations in the bottom bed region are faster than the response time of this type of sensor.

Keywords: Circulating fluidised bed boiler; CFB; Zirconia cell sensor

1. Introduction

To improve the understanding of the combustion process in fluidised bed furnaces it is advantageous to consider the fluctuating properties of the fluidised medium, such as temperature, gas concentrations, velocity and particle loading. The severe environment and the rapid variation of the conditions inside a furnace make measurements of such quantities difficult, however. One method to study fluctuating gas concentrations is by zirconia cell sensors inserted into the furnace, e.g. [1–8]. Zirconia cell sensors have been produced in millions to control the air to fuel ratio in car engines, where the sensor measures the air ratio in the exhaust gas. The measurement technique has the advantage of being simple and cheap, with reasonably short response time.

Unfortunately, the interpretation of the output voltage signal is not straightforward when the sensor is exposed to fluctuating conditions in a fluidised bed combustor. In an ideal case, where the sample gas consists of only inert gas, combustion products and oxygen, the voltage signal (U) is correlated to the partial pressure of oxygen (P_{O_2}) in the gas according to the Nernst equation

$$U = \frac{RT}{4F} \ln\left(\frac{P_{O_2}(\text{ref})}{P_{O_2}(\text{sample})}\right) \quad (1)$$

where R is the universal gas constant, T the temperature of the cell and F the Faraday's constant. When the combustion is still in progress, some gas components (such as H_2, CO and hydrocarbons) may interact with the oxygen on the catalytic surface on the sample side, whereby the voltage signal is affected. Since the electrode surface is highly catalytic (it is covered by a porous platinum layer), it has been argued that thermodynamic equilibrium of the sample gas is established on the surface, and that the voltage signal of the sensor is determined by the equilibrium partial pressure of oxygen [6]. If so, it follows from Eq. (1) that the signal shows a steep change around the stoichiometric gas composition [9].

In practice, there is a slotted metal shield surrounding the cell and inside this shield the gas has to diffuse through a protective coating made of porous magnesium-spinel, before reaching the catalytic platinum layer. Since the diffusivities of gas species differ from each other (especially H_2 differs from oxygen), the oxygen concentration at thermodynamic equilibrium on the platinum surface may be different from the one in the sample gas. The influence on the voltage signal by a range of gas components has been investigated by Rau and Schwartz [10] and Brailsford et al. [9], who also gave corrections on the Nernst equation for these gas components. Furthermore, it has been shown that sensors from different manufacturers give different responses to the air to fuel ratio when the sample gas contains, for example, hydrogen [11]. This effect is probably due to the properties

* Corresponding author. Tel.: +46-31-772-1438; fax: +46-31-772-3592.
E-mail address: frni@entek.chalmers.se (F. Niklasson).

1385-8947/$ – see front matter © 2003 Elsevier B.V. All rights reserved.
doi:10.1016/j.cej.2003.08.020

Nomenclature

B	transition voltage level (V)
C_F	gaseous fuel concentration (volume fraction)
C_{O_2}	oxygen concentration (volume fraction)
C_β	virtual oxygen concentration (volume fraction)
E	gas exchange rate (s^{-1})
f_{ox}	time fraction at oxidising condition (–)
f_{red}	time fraction at reducing condition (–)
F	Faraday's constant (9.65×10^4) (A s/mol)
g_{0t}	stoichiometric flue gas yield per mass unit of fuel (m^3/kg)
h	height above air distributor (m)
k	index of phases: (1) oxidising; (2) reducing (–)
K	empirical parameter (–)
l_{0t}	stoichiometric air demand per mass unit of fuel (m^3/kg)
m_{loc}	local air ratio (–)
n_f	average frequency of fluctuations (Hz)
P_{O_2}	partial pressure of oxygen (Pa)
R	universal gas constant (8.314) (J/(mol K))
$S_{\beta,k}$	source term of C_β (volume fraction/s)
t	time (s)
t_{ox}	average duration of oxidising pulses (s)
t_{red}	average duration of reducing pulses (s)
T	temperature of zirconia cell (K)
U	voltage signal from zirconia cell (V)
U_k	superficial gas velocity of phase k (m/s)

Greek symbols

γ	oxygen demand of gaseous fuel (mol oxygen/mol fuel) (–)
μ, σ	empirical parameters used in Eq. (5) (–)
τ	time constant of zirconia cell sensor (s)

of the protective coatings. Thus, corrections may have to be applied on Nernst equation to measure the oxygen concentration in different atmospheres, but this requires that the corrections are verified for the particular sensor in use and that the concentrations of a range of gas species are known in the gas measured. In a fluidised bed furnace, there is usually insufficient information on the fluctuating gas concentrations to apply such corrections. Furthermore, vivid fluctuations of gas concentrations in a fluidised bed furnace could prevent equilibrium to be established on the catalytic surface, and the gas composition may not be the same over the whole sensor. Therefore, under these conditions, the partial pressure of oxygen derived from Nernst equation is unreliable. The equation shows that there could also be an influence of temperature. However, thermocouple measurements show that, on the time scale considered, temperature fluctuations in the bed are small in relation to the response of the zirconia cell probe. Also the influence of changes in heat transfer because of variations in particle concentration is negligible thanks to the protective outer metal shield.

Since the actual oxygen concentration is difficult to extract accurately from the voltage signal of the zirconia cell sensor in a fluidised bed furnace, previous work instead focussed on the time fractions under reducing or oxidising conditions [1–3,7,12,13], which for some applications are of more interest than the average oxygen concentration:

- The time fraction under reducing conditions in different locations in a fluidised bed furnace can be used to determine the potential risk of in-bed corrosion [2,6,12].
- The frequency of fluctuations and the average time intervals under reducing or oxidising conditions has been shown to be important for sulphur capture by limestone in fluidised bed firing coal [7,14,15].
- The time fractions under reducing condition may vary over the cross-section in the furnace, indicating lateral maldistribution of fuel and air, which reduces the performance of the combustor [13,16].
- Fluctuations from zirconia cell sensors have also been used, with moderate success, to study properties of bubbles in the bed [3,6].

Statistical properties of fluctuations in zirconia cell signals are easily captured and are not sensitive to the exact correlation between oxygen concentration and voltage signals when they only differentiate between two states (reducing or oxidising). To distinguish oxidising from reducing conditions, the voltage levels of reducing and oxidising conditions have to be determined. Holt et al. [17] suggested a partial pressure of oxygen above 10^{-3} bar to be oxidising and below 10^{-12} bar to be reducing atmosphere. These limits are chosen somewhat arbitrarily, but the limit is not critical as long as it is well within the range of the fluctuations, because the voltage signal swiftly changes between high and low values.

In summary, the zirconia cell probe has been proven to be a robust in situ measurement technique for use in fluidised bed combustors. The interpretation of the results is not clear, however, and it has not been reported how the properties of the fluctuating signal depend on the local air ratio of the flue gas. Therefore, the aim of the present work is to establish a correlation between the time fractions under reducing or oxidising conditions, measured by a zirconia cell sensor, and the local air ratio in the gas of a fluidised bed furnace, measured by a suction probe and conventional gas analysers. The present analysis is valid for conditions in the furnace that do not deviate too far from stoichiometric conditions so that fluctuations between oxidising and reducing conditions occur.

1.1. The zirconia cell

The vital part of a zirconia cell sensor is the electrochemical layer made of stabilised zirconium oxide, which

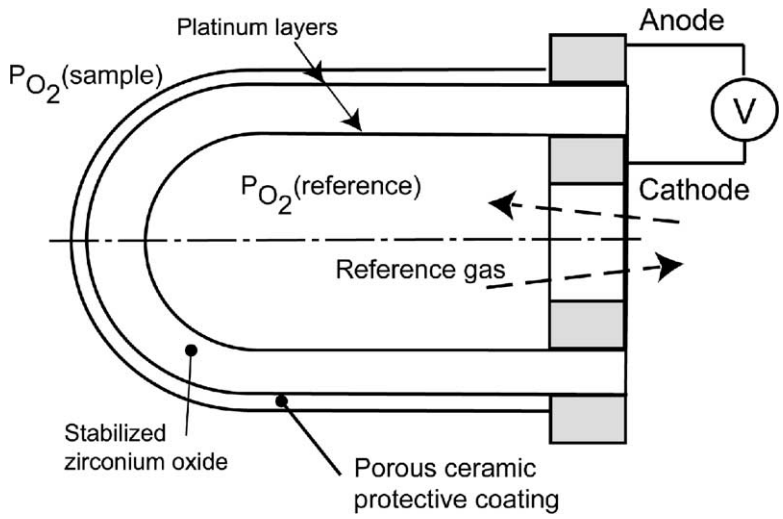

Fig. 1. Schematics of a zirconia cell sensor. The sample gas is outside the thimble shaped zirconium oxide layer and reference gas on the inside. Oxygen ions formed at the cathode migrate through the medium, which gives a voltage between the two surfaces. The protective slotted metal shield surrounding the cell is omitted in the figure.

is doped to create defects of the atomic structure, leaving voids where oxygen ions can migrate through the material if the temperature is sufficiently high (in the order of 600 °C). The cell material is a selective oxygen ion conductor. The schematic of a zirconia cell sensor is outlined in Fig. 1. Porous platinum plates, used as electrodes, cover the surfaces of the zirconia material. The inner reference side is usually flushed with air serving as a reference gas. If the partial pressure of oxygen differs in sample and reference gas, oxygen atoms are ionised at different rates on the surfaces, and the ions diffuse through the ion conductor, giving rise to a voltage between the electrodes that is determined by the difference of partial pressure of oxygen across the cell. The voltage formed is the output signal from the sensor.

The sensors used in this work were manufactured by Bosch and are thimble shaped, 24 mm long and 8 mm in diameter. An external slotted stainless steel shield (omitted in Fig. 1) together with a porous ceramic coating on the catalytic surface protect the cell from erosion and corrosion. Further description of the Bosch zirconia cell sensor is given by Saari and Davini [6] and Bergqvist [1]. The zirconia cell sensor was mounted at the tip of a probe that is water-cooled, except for the 10 cm closest to the cell, where air cooling is applied in order to avoid large temperature gradients within the cell. Three of these probes were used simultaneously in the measurements, inserted into the centre of the furnace at different heights. The voltage signals were logged at a sampling rate of at least 20 Hz during 180 s. It has been shown previously that higher sample frequency adds no further information, since the response time of this zirconia cell sensor, under fluidised bed conditions, is in the order of 0.05 s, probably limited by the gas diffusion through the protective coating [1].

2. Method

2.1. Local air ratio

To avoid introduction of a large number of unknown gas concentrations and to simplify the discussion when studying the voltage signal from the sensor in a combustion chamber, a virtual oxygen concentration, C_β, is introduced as

$$C_\beta = C_{O_2} - \gamma C_F \tag{2}$$

where C_{O_2} is the actual oxygen concentration and C_F the total concentration of combustible gases (only CO and hydrocarbons are considered here), which consumes γ moles of oxygen per mole of fuel gas. This virtual oxygen concentration becomes negative under reducing conditions. It is used to estimate a local air ratio (m_{loc}) as

$$m_{loc} \approx 1 + \frac{g_{0t}}{l_{ot}} \frac{C_\beta}{0.21 - C_\beta} \tag{3}$$

where g_{0t} is the gas yield from stoichiometric combustion (per unit mass of fuel) and l_{0t} the corresponding air demand. The overall average air ratio is given by the flow of air to the combustor divided by the stoichiometric air demand of the fuel, whereas m_{loc} is an estimation of the condition of the gas in a particular point. m_{loc} differs from the overall air ratio by the unburnt fuel that remains in solid phase at the point of measurement. Since the zirconia cell sensor responds only to the conditions of the gas, it is preferable to correlate its output signal to m_{loc} and not to the overall average air ratio. The local air ratio in the centre of the furnace may differ from the overall average air ratio also if there are lateral gradients of oxygen and combustible gases. This uncertainty, when correlating the conditions of the gas to the signal from the zirconia cell, is circumvented by estimating m_{loc} from gas

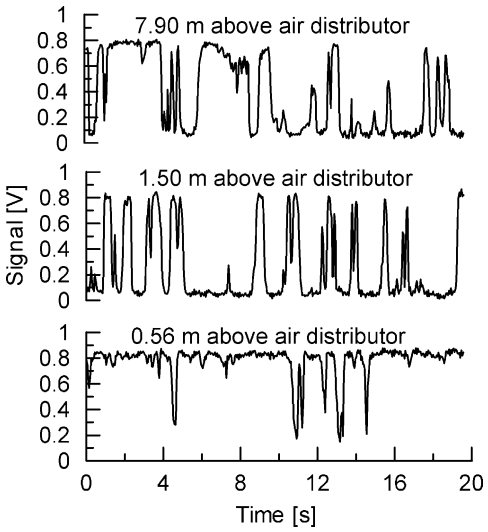

Fig. 2. Simultaneous voltage signals from zirconia cell probes at different heights in the CFB furnace when firing coal and $m_{loc} \approx 1$. No secondary air was supplied.

concentrations measured in the same position as the zirconia cell sensor.

The voltage signal from a zirconia cell sensor inserted into a fluidised bed furnace usually fluctuates between two almost saturated states, as illustrated in Fig. 2. (The experimental conditions and the plant are described in the next section.) The values of the voltage signals, such as shown in Fig. 2, are summarised in the form of probability density functions in Fig. 3, showing that the signal seldom is between 0.3 and 0.6 V. When the voltage is below this transition region, the condition of the gas is oxidising ($C_\beta > 0$), and when the voltage is higher, the condition is reducing ($C_\beta < 0$). Here, for convenience, the two states will be separated by a voltage level of $B = 0.4$ V.

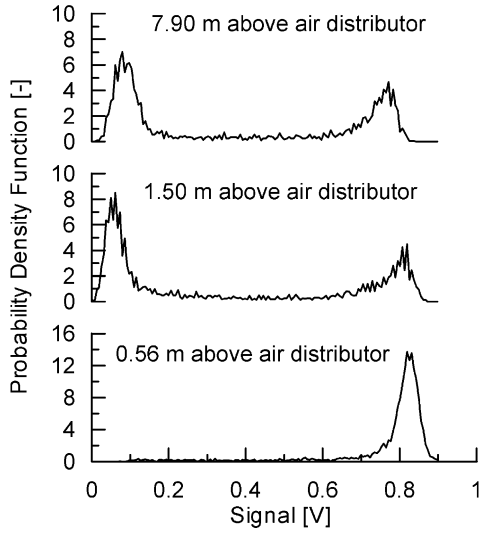

Fig. 3. Probability density functions of the voltage signals of Fig. 2.

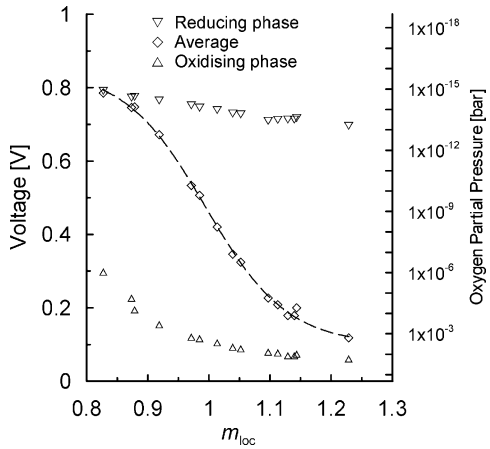

Fig. 4. Voltage signal under reducing and oxidising conditions and the average value at 7.90 m above the air distributor, when firing wood chips in a CFB.

The voltage signal depends on the gas components and on whether thermodynamic equilibrium is established on the surface of the zirconia cell. The average voltage, on the other hand, mainly depends on the time fractions, during which the zirconia cell is exposed to each of the two phases. An example of the average voltage signal from a zirconia cell sensor at 7.9 m above the air distributor, when firing wood, is shown as a function of m_{loc} (defined by Eq. (3)) in Fig. 4. The voltage signal (U) is split into three average voltages indicating: the time under reducing conditions ($U > B$), under oxidising conditions ($U < B$) and the average of the signal during the total time. The average voltage of each phase (oxidising or reducing) changes little with m_{loc} compared to the total time-average signal, which mostly depends on the time fractions of each phase. The fraction of time that the voltage signal is below the transition level is called f_{ox}. The dependence of f_{ox} on m_{loc} is illustrated in Fig. 5, which shows a behaviour that is similar to the average

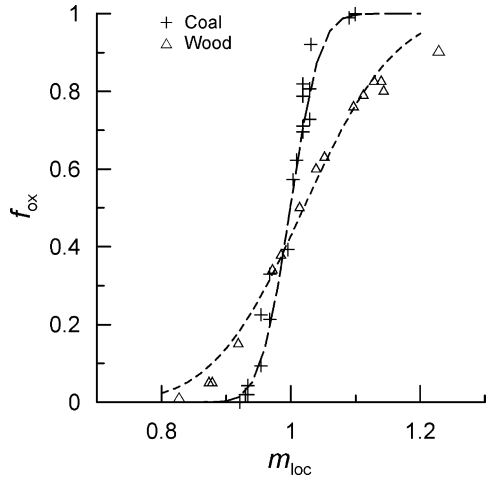

Fig. 5. Time fraction of oxidising condition (f_{ox}) vs. the local average air ratio (m_{loc}) at a height of 7.9 m above the air distributor when firing wood chips or coal.

voltage signal in Fig. 4, but the advantage is that f_{ox} varies between two known levels (0 and 1). The average voltage signal can be replaced by f_{ox} without any significant loss of information in the presence of two clearly distinguished phases.

The variation of f_{ox} with the local air ratio can be represented by some simple function expressing its position and slope. Such a function could be, for instance, the error function

$$\mathrm{erf}(x) = \frac{2}{\sqrt{\pi}} \int_0^x \mathrm{e}^{-t^2}\,\mathrm{d}t \tag{4}$$

which goes from -1 to 1 symmetrically around $x = 0$. In the present case the function looks like

$$f_{ox} = \frac{1}{2}\left[1 + \mathrm{erf}\left(\frac{m_{loc} - \mu}{\sigma}\right)\right] \tag{5}$$

where μ determines the position and σ the slope of the curve at the position $m_{loc} = \mu$,

$$\frac{\partial f_{ox}}{\partial m_{loc}} = \frac{1}{\sqrt{\pi}\sigma} \tag{6}$$

The local air ratio m_{loc} can be expressed as a weighted average of the two phases

$$m_{loc} = f_{ox} m_{loc,2} + (1 - f_{ox}) m_{loc,1} \tag{7}$$

where $m_{loc,2}$ and $m_{loc,1}$ are the local air ratios of respective phases, given the indices (1) for the reducing phase and (2) for the oxidising phase. Here, the transition time between oxidising and reducing conditions is neglected, which gives that $f_{ox} + f_{red} = 1$. The measured average local gas concentrations give m_{loc} and zirconia cell measurements give f_{ox} (and f_{red}), but the local air ratios of the two phases are unknown. To estimate these, the derivative of m_{loc} with respect to f_{ox} (Eq. (8)) can be used together with Eq. (7):

$$\frac{\partial m_{loc}}{\partial f_{ox}} = m_{loc,2} - m_{loc,1} \tag{8}$$

The derivative can be estimated from experiments, where f_{ox} is measured in a point in the combustion chamber during changes of the local air ratio, similar to what was shown in Fig. 5. Eq. (8) shows that, the smaller the difference between the local air ratios of the phases, the lower becomes σ and the steeper is the slope of the curve expressed by Eq. (5).

The presence of two clearly separated gas phases in the combustion chamber indicates that the gas phase reaction rate is limited by large-scale mixing rather than by chemical kinetics. This observation can be used to assess the trend of σ along the height (h) in the freeboard region, from mass balance on horizontal segments of the furnace under stationary conditions. The gas flow is divided into two phases: the reducing phase ($k = 1$), which is assumed to contain gaseous fuel but no available oxygen, and the oxidising phase ($k = 2$), which contains oxygen but no gaseous fuel. What is mixed is assumed to burn instantly. The virtual oxygen concentration, $C_{\beta,k}$, defined in Eq. (2), gives that $C_{\beta,1} < 0$ and $C_{\beta,2} > 0$ if both gaseous fuel and oxygen remain in the fluid. The mass balance of $C_{\beta,k}$ is formulated as

$$-\frac{\partial}{\partial h}(U_k C_{\beta,k}) + S_{\beta,k} + (-1)^k E(C_{\beta,1} - C_{\beta,2}) = 0 \tag{9}$$

where U_k is the superficial gas velocity of phase k, $S_{\beta,k}$ is a source term that accounts for production/destruction from combustion and E the gas exchange rate, which is assumed constant with height and the same in both directions, whereby the net gas exchange rate is zero. To further simplify the derivation, no solid fuel conversion is accounted for and constant superficial gas velocities are assumed. As a consequence of the definition, C_β remains unaffected by combustion of gaseous fuel, which implies that S_β is equal to zero and that C_β is a conserved scalar. These simplifications of Eq. (9) result in

$$\frac{\partial C_{\beta,k}}{\partial h} = (-1)^k \frac{E}{U_k}(C_{\beta,1} - C_{\beta,2}) \tag{10}$$

The difference between the two phases yields a first-order linear differential equation

$$\frac{\partial}{\partial h}(C_{\beta,2} - C_{\beta,1}) = -E\left(\frac{1}{U_1} + \frac{1}{U_2}\right)(C_{\beta,2} - C_{\beta,1}) \tag{11}$$

which has the solution

$$(C_{\beta,2} - C_{\beta,1}) = K_1 \exp\left[-E\left(\frac{1}{U_1} + \frac{1}{U_2}\right)h\right] \tag{12}$$

where K_1 is a constant that depends on the boundary conditions. In order to find a simple relationship between σ and height, the derivation is restricted to a case in the vicinity of $m_{loc} \approx \mu \approx 1$, where the derivative of Eq. (5) is proportional to $1/\sigma$ and as follows from Eq. (8), $m_{loc,2} - m_{loc,1}$ is proportional to σ. In addition, the difference between the local air factors $m_{loc,2} - m_{loc,1}$ is almost proportional to $C_{\beta,2} - C_{\beta,1}$ (from linearisation of Eq. (3)) when $C_{\beta,1} + C_{\beta,2} \approx 0$ (i.e. $m_{loc} \approx 1$). These two linearisations together with Eq. (12) give a correlation as

$$\sigma = K \exp\left[-E\left(\frac{1}{U_1} + \frac{1}{U_2}\right)h\right] \tag{13}$$

where K is an empirical parameter. This estimation shows an exponential decline of σ with height.

If the average air ratio is far below unity, or if all fuel is burnt, all of the gas may become either reducing or oxidising, and f_{ox} is either 0 or 1. In both cases the derivative in Eq. (8) approaches zero, and the furnace is better described as a perfectly mixed reactor. In such a case, this evaluation method based on two different phases is no longer applicable. Experiments were performed to find out how the properties of the fluctuating signals from zirconia cell sensors depend on the height above the bed, the fuel properties, and the air to fuel ratio.

3. Experiments

3.1. The boiler

Zirconia cell measurements were performed in the Chalmers 12 MW circulating fluidised bed (CFB) boiler, outlined in Fig. 6 and further described in [7,18], although all necessary information is given below. Also the data of Figs. 2–5 were obtained from this plant. The size of the combustion chamber is 1.7 m × 1.7 m × 13.5 m. The fluidisation air is introduced through 144 air-cap nozzles that form the air distributor. The vertical walls are covered with refractory lining (0.11 m thick) up to 2 m above the air distributor and two of the walls are covered all their height. The average height of the dense bottom bed was estimated to be about 0.5 m. The fuel enters the combustion chamber by gravity from the fuel chute, (2) in Fig. 6, at a height of 1.1 m above the air distributor. Entrained bed material is captured in the refractory lined cyclone (5) and returned to the combustion chamber by the particle seal (6). The bed temperature is controlled by an external heat exchanger at the particle seal (7) and by recycled flue gas, which is mixed with the primary air below the air distributor.

The tests involved variation of the air ratio in the fluidised bed furnace. Normally, secondary air is injected into the furnace somewhere above the bed, but here, in order to maintain the same total air ratio in the whole riser, the secondary air was injected at the exit of the cyclone (at 4 in Fig. 6). The ratio of secondary to primary air was varied from zero to about 0.7 and the fuel feed rate was adjusted to always maintain an oxygen volume concentration of 3.5% in the stack. With the intention to change the conditions of the fluid dynamics in the furnace as little as possible between the test cases, the boiler was operated with a primary airflow of about 2.1 kg/s in all test cases at a bed temperature of 830–860 °C. The average pressure drop over the bed was about 6 kPa and the dominant bubble frequency was about 1–2 Hz, estimated from pressure fluctuations in the bed. The boiler operation parameters and the fuels are specified in Table 1. Three fuels were fired: (A) wet wood chips, (B) Russian bituminous coal and (C) British bituminous coal. In the context of the present tests, the coals were similar and no differentiation is made between them.

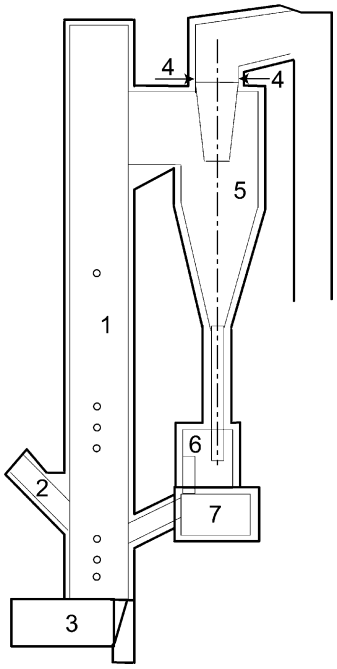

Fig. 6. The 12 MW CFB boiler at Chalmers University of Technology: (1) combustion chamber; (2) fuel feed chute; (3) air plenum; (4) secondary air inlet into cyclone exit duct; (5) cyclone; (6) particle seal; (7) heat exchanger. Measurement ports on the boiler wall indicated as circles.

Table 1
Boiler operation parameters

	Wood chips	Coal (Russian)	Coal (British)
Primary gas flow (kg/s)	2.0–2.2	2.0–2.3	2.0–2.3
Secondary air flow (kg/s)	0.17–0.70	0–0.69	0–0.69
U_{mf} (m/s)	0.03	0.03	0.03
U_{tot} (m/s)	3.7–4.4	3.3–3.9	3.3–3.9
Bed pressure drop (kPa)	5–6	5–6	5–6
O_2 at stack (vol.%, dry gas)	3.0–3.7	2.9–3.5	2.9–3.5
Fuel (kg/s)	0.58–0.87	0.29–0.43	0.29–0.43
Bed temperature (°C)	830–860	830–860	830–860
Bed material	Silica sand	Silica sand	Silica sand
Size (mm)	0.30	0.30	0.30
Fuel analysis			
Moisture (%)	46	11.2	14.1
Volatiles (%)	44	29.5	30.4
Ash (%)	0.3	11.6	6.9
C_{fix} (%)	10	47.7	48.6
S (%)	–	0.38	1.33
Lower heating value[a] (MJ/kg as-received)	9.0	24.7	25.7

[a] Estimated from fuel composition.

3.2. Gas measurements

Boiler operation parameters, such as flow rates, temperatures and pressures, were monitored and logged once a minute. Gas concentrations of O_2, CO, CO_2 and hydrocarbons were measured on-line in the combustion chamber by a water-cooled gas suction probe, which was inserted into the centre of the furnace at 4.2 or 7.9 m above the air distributor. The gas sample was pumped through the probe, having a ceramic filter at the tip, via tubing to a gas drier and a set of gas analysers, which were calibrated regularly. The hydrocarbon instrument measured the total concentration of hydrocarbons as methane equivalents by a flame ionisation detector (FID). The gas was usually sampled during 5–10 min in every measurement before the filter was cleaned by back-blowing pressurised air through the probe.

4. Results and discussion

The zirconia cell signal depends on the position in the furnace, on the fuel properties and on the local air ratio. In the region close to the surface of the bed (0.56 m in Fig. 2), the voltage signal showed almost constant reducing conditions, while at the next level (1.50 m), the signal was vividly fluctuating between high and low voltage levels. This behaviour is a consequence of the high gas velocity of the intermittent gas jets of the oxidising phase from eruptions of bubbles, implying that the measurement probe close to the bed's surface was exposed to oxidising conditions during short time intervals, often shorter than the response time of the zirconia cell. Thus, the response time is not always short enough to catch the dynamics in the bed region of a CFB boiler, but it can still be used further up in the furnace, where the difference between the gas velocities of the phases is reduced.

The problem of uneven gas velocities of the phases in the region close to the bed remains the same when measuring the gas concentration by extraction of gas samples to on-line gas analysers. To determine the global average from a measurement in a fixed point, the gas velocity should be measured at the same time as the gas concentration; otherwise the measured average is biased towards the concentration of the gas with lowest velocity. However, a few meters above the bottom bed, in the freeboard, the difference of gas velocities of the phases is small, and the measured gas concentration represents the average value of the gas flow. The measured average local gas concentrations of O_2, CO and hydrocarbons at 7.9 m above the air distributor are shown in Fig. 7, plotted against the average air ratio, m_{loc}, which was altered by varying the fuel feed rate together with the secondary air supply, and calculated from Eqs. (2) and (3).

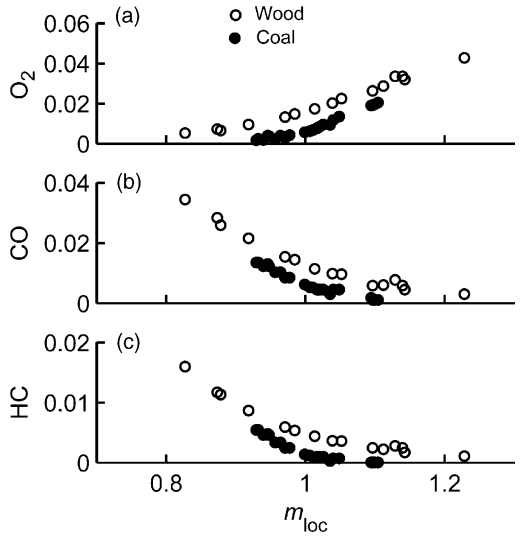

Fig. 7. Measured gas concentrations (dry gas) at 7.9 m above the air distributor vs. local air ratio when firing wood chips or coal: (a) oxygen; (b) carbon monoxide; (c) hydrocarbons as methane equivalents.

The difference between the gas concentrations of wood and coal indicates that the coal burns to a larger extent in the lower region of the furnace. The gas concentration measurements were performed in the freeboard of the furnace, while the fuel particles mostly devolatilise in the bed region before being fragmented into small pieces that may become entrained. This results in unburnt carbon in the form of fine char that is present in a low concentration along the entire height of the furnace. Since no air or fuel was introduced into the combustion chamber between the fuel chute and the exit, the global air ratio was constant along the riser from the fuel injection until the exit to the cyclone. However, the char that is consumed along the height affects to some extent the local air ratio of the gas, estimated by Eq. (3), which does not account for the solid fuel present. In addition, products of devolatilisation influence the local air ratio of the gas, particularly in the bed or splash zone. Therefore, the estimation in Eq. (3) is suitable above the bed and splash zone only, where the presence of devolatilisating fuel particles is small and the combustion rate of entrained char particles is limited.

The measured time fractions under oxidising conditions (f_{ox}) from zirconia cell measurements at different heights and varied air ratios were compared to m_{loc} in order to estimate the parameters μ and σ in Eq. (5). The results at 7.9 m above the air distributor are illustrated in Fig. 5 and at different heights when firing wood in Fig. 8, where the symbols are measurements and the lines are the correlation, Eq. (5). μ was in the range of 0.99–1.02 when the gas concentration and the zirconia cell measurements were performed at the same height. The function described by Eq. (5) may be affected when m_{loc} is determined from a gas concentration measurement at another height than f_{ox}, if gas production from the solid fuel alters the air to fuel ratio of the gas between the two positions. Such a displacement of the gas concentration measurement prevented accurate determination of μ in the lower positions of the furnace in the present

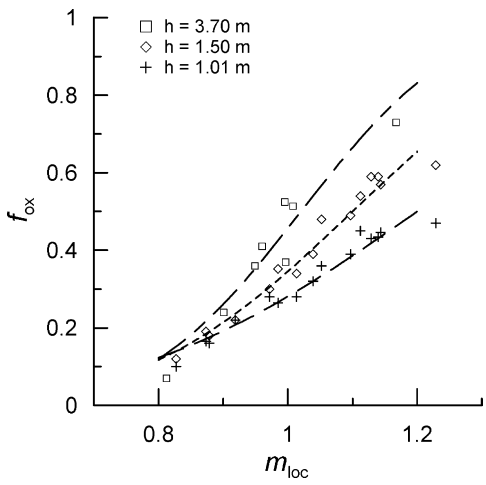

Fig. 8. Time fraction of oxidising condition (f_{ox}) vs. local average air ratio (m_{loc}) at different heights above the air distributor.

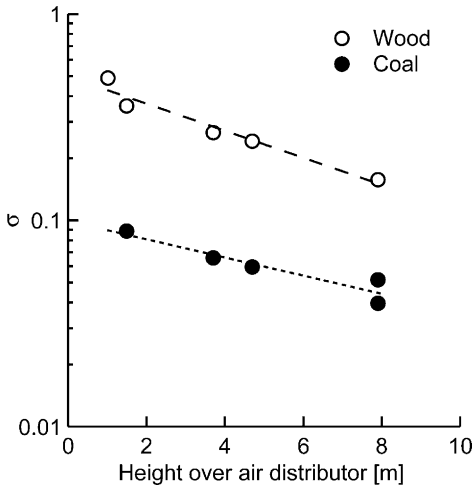

Fig. 9. Estimated values of σ along the height of the furnace; the symbols are from a curve fit of Eq. (5) to measured data and the trend lines are from the exponential function in Eq. (13), with parameters adjusted to fit the data points.

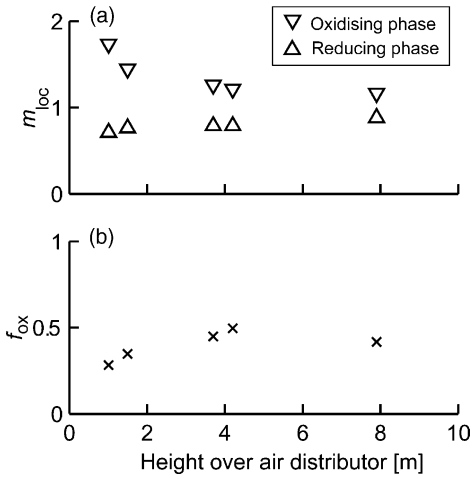

Fig. 10. (a) Development of m_{loc} in oxidising and in reducing phases using Eqs. (7) and (8) along the height of the furnace under stoichiometric conditions; (b) f_{ox} in the same case.

experiments. The effect of the displacement is estimated to be less than 10% in the freeboard, where it is caused by combustion of fine char particles. This is not a consequence of the method as such, as long as the gas concentrations are measured at the same position as the zirconia cell or when there is no gas production from solid fuel between the cell and the sampling for gas analysis. Although there was a displacement of the curve in the present case, it has only a small influence upon the slope, σ. This parameter, determined from the experiments, is plotted against the height of the combustion chamber in Fig. 9. σ follows a clear trend; it is reduced with height and it shows a lower value for coal than for wood. The trend along the height is well described by an exponential fit, in accordance to Eq. (13), which gives the dashed lines in Fig. 9. The lower values of σ for coal than for wood chips, under globally similar conditions, is obviously due to the larger volatile fraction in wood than in coal and earlier combustion when using coal, which to a large extent burns in the bed, in contrast to wood, whose large volatile fraction mostly burns above the bed. The volatiles are less mixed with the oxidising phase than the products of partial combustion of char. Consequently, the gas mixing in the freeboard is more critical for high volatile fuels than for fossil fuels.

The gases of the two phases interact and burn while the gas flows upwards in the combustion chamber, which reduces the difference between the local air ratios of the two phases, gives a steeper relationship between f_{ox} and m_{loc} in Fig. 8, and a trend of falling σ in Fig. 9. The somewhat faster fall of σ with height when firing wood compared to coal may indicate that the gas exchange rate (E) is higher in the wood case where more combustible gases are present. Even though the trend in Fig. 9 probably is general, the parameters of the relationship depend on the fuel and on the rate of mixing between the two phases, which, in turn, depends on the geometry of the furnace and on the conditions of fluidisation.

The average local air ratios, in each of the two phases, can be estimated from the test results by Eqs. (7) and (8). The local air ratios are plotted against the height of the furnace in Fig. 10a at the average air ratio of $m_{loc} = 1$. The values of f_{ox} and dm_{loc}/df_{ox} at $m_{loc} = 1$ were calculated using Eq. (5). The local air ratios of the two phases approach the asymptotic value of the given average air ratio (1, in this case) with increasing distance from the dense bed. The local air ratio of the oxidising phase decreases faster than that of the reducing phase is increased, because the oxidising regions above the bed expand, extending the time fraction of the oxidising phase in the lower part of the riser, as seen in Fig. 10b, where f_{ox} is plotted against height. At an average local air ratio of unity and f_{ox} less than 0.5, Eq. (7) gives an oxygen concentration in the oxidising phase that is higher than the oxygen demand (per volume unit) from the gaseous fuel in the reducing phase, i.e. $C_{\beta,2} > |C_{\beta,1}|$. This situation probably originates from the two-phase flow in the bed, where the oxidising phase (oxygen rich bubbles) occupies a considerably smaller volume fraction than that of the reducing phase (surrounding emulsion). Above the surface of the bed, the oxidising regions expand with height and their velocities are reduced to become more equal to that of the reducing phase.

4.1. Fluctuations

The average frequency of change between the two phases has been extracted from the measurements at different heights and different local air ratios. The average fluctuation frequency (n_f) is plotted against the average time fraction of oxidising conditions (f_{ox}), for wood chips in Fig. 11, and for coal in Fig. 12. The highest fluctuation frequency was

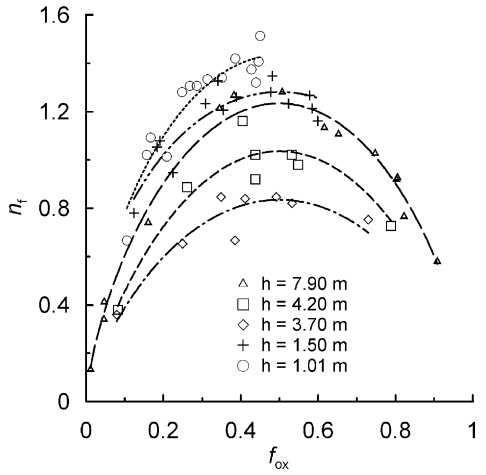

Fig. 11. Average frequency of fluctuations, firing wood.

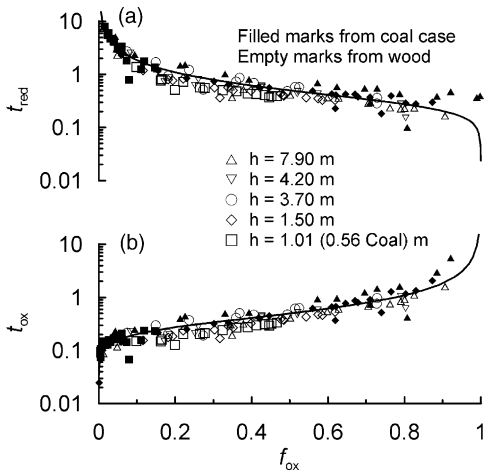

Fig. 13. Average duration of fluctuations (in s): (a) reducing periods; (b) oxidising periods, in log-scale.

found in the lower part of the combustion chamber around $f_{ox} = 0.5$. The maximum fluctuation frequency is in the same order of magnitude as the dominant bubble frequency (1–2 Hz) and one could suspect that the distinction of the medium in oxidising and reducing phases is linked to the eruptions of bubbles at the surface of the bottom bed. As can be seen from Fig. 11, the maximum of the fluctuation frequency is gradually reduced along the height of the combustion chamber, up to 4 m, but then the frequency of fluctuation increases from 4 to 7.9 m for wood (Fig. 11), but not for coal (Fig. 12). This difference between the fuels cannot be explained at present.

The measured average duration of fluctuations in each phase, t_{ox} for the oxidising phase and t_{red} for reducing conditions, is plotted in Fig. 13, for test series utilising both coal and wood fuels and at various heights. Since the time fraction of oxidising conditions (f_{ox}) should be equal to the fluctuation frequency times the average duration of each fluctuation, the parabolic curves in Figs. 11 and 12 can be used to estimate the average duration of each oxidising packet from

$$t_{ox} = \frac{f_{ox}}{n_f} \tag{14}$$

which is plotted as the solid line in Fig. 13b. The trend represents well the data, and the times of the oxidising regions are strongly related to f_{ox}. The average duration of the reducing periods is estimated similarly, simply by changing the numerator f_{ox} in Eq. (14) to $(1 - f_{ox})$, and is shown as the solid line in Fig. 13a. From the fluidisation velocities in Table 1 it can be deduced that a time of 0.5 s corresponds to a length of a gas packet of about 2 m.

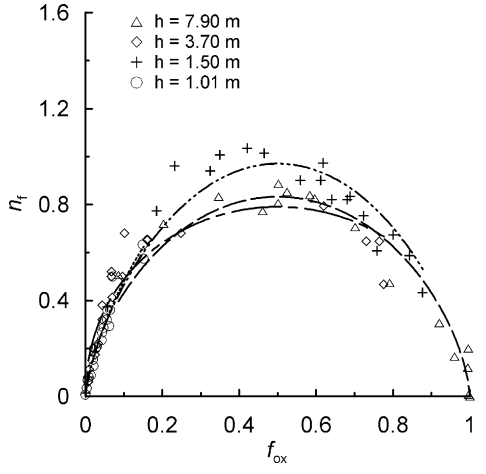

Fig. 12. Average frequency of fluctuations, firing coal.

4.2. Measurement performance

Fluctuations of shorter duration than the response times of the zirconia cell sensors (about 0.05 s) cannot be detected, and regions with a vertical size of less than 0.2 m can pass the sensor undetected when the average gas velocity is higher than about 3.5 m/s. It is likely that more shifts would have been detected if the response time of the sensor was shorter. Then the frequency of fluctuations, Figs. 11p3pcand 12, would be higher and the cycle times in Fig. 13 would be shorter. Hence, only large-scale fluctuations are captured from measurements with zirconia cell sensors. This is illustrated in Fig. 14, which shows modelled voltages (dashed fat line) from a sensor exposed to an atmosphere that fluctuates stepwise between oxygen partial pressures of 10^{-15} and 10^{-1} bar (thin solid line). The voltage from the sensor (U) is characterised as

$$\frac{dU}{dt} = -\frac{1}{\tau}(U - U_a) \tag{15}$$

where U_a is the voltage from an ideal sensor, calculated from Eq. (1) at the ambient partial pressure of oxygen, and τ the time constant of the sensor (a value of $\tau = 0.08$ s was used in the illustrations). In Fig. 14a, the atmosphere is assumed to fluctuate symmetrically ($f_{ox} = 0.5$) with a

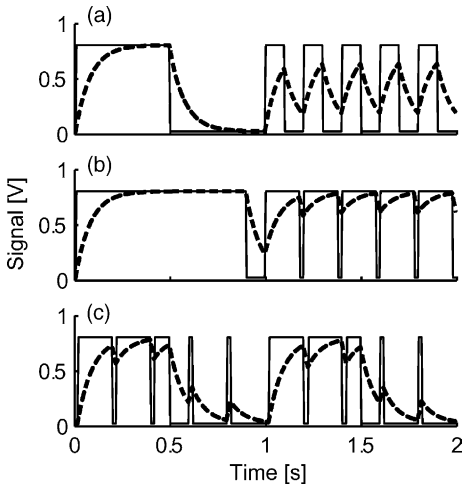

Fig. 14. Signal from an assumed binary fluctuating atmosphere. The thin solid line is for an ideal sensor with infinitely fast response time and the dashed line is the signal from a sensor with a time constant of 0.08 s.

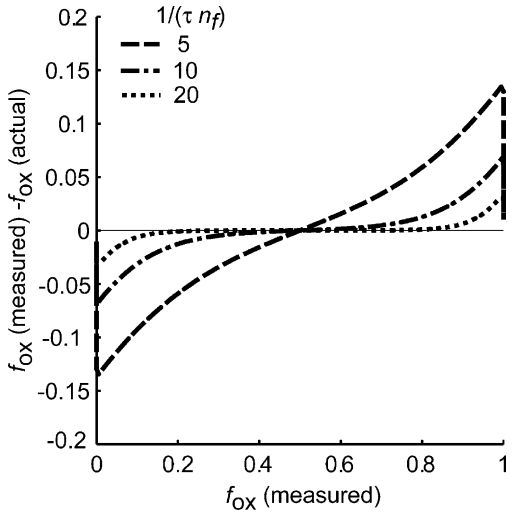

Fig. 15. Difference of detected and actual f_{ox} from assumed fluctuations and modelled response, as illustrated in Fig. 14, for different ratios of the period of fluctuations and response time of the sensor ($(1/n_f)/\tau$).

frequency of 1 Hz during the first period and later at 5 Hz. The signal of the sensor tends to approach an intermediate value when the frequency of the symmetric fluctuations becomes high (>5 Hz). Such intermediate voltages are seldom observed in measurements from fluidised bed boilers, and it can be concluded that the dominant frequency is not higher than the one measured. However, for inhomogeneous fluctuations, for example at $f_{ox} = 0.10$, as shown in Fig. 14b, the oxidising periods are on an average much shorter than the reducing periods. In this case it is likely that several oxidising periods pass the sensor undetected; the signal from the sensor underestimates f_{ox} under highly reducing conditions. The situation is reversibly similar under highly oxidising conditions, where the sensor would overestimate f_{ox}. Thus, the method to estimate the time fractions of reducing/oxidising atmospheres from zirconia cell measurements is most reliable around $f_{ox} = 0.5$, and the reliability becomes lower with distance from this value. Furthermore, in case of $f_{ox} = 0.5$, superimposed faster fluctuations may be present, and there could be smaller regions of oxidising gas escaping detection in an overall reducing period, and vice versa in the oxidising periods, as illustrated in Fig. 14c. However, such small-scale fluctuations have a small influence on the overall estimation of f_{ox} if they exist in both phases, and only the large-scale (dominant) fluctuation frequency is detected.

The errors of the measured f_{ox} are estimated in Fig. 15, and expressed as the difference in time fraction under oxidising conditions of assumed binary signals and calculated output signals, such as in Fig. 14. The estimations were made for various ratios of fluctuation period ($1/n_f$) and response time of the sensor (τ). In our case, with a frequency of fluctuation of around 1 Hz and a response time of about 0.05 s, the ratio is in the order of 20, for which Fig. 15 shows that the error is small in the interval of $0.15 < f_{ox} < 0.85$. This analysis, based on binary fluctuations, is a simplification compared with the distributions of sizes of gas packets and gas compositions of the real gas in the furnace, but it gives a clear indication on the accuracy.

5. Conclusions

The local air ratios of a combustion chamber burning solid fuel are evaluated with a method that is applicable to full-scale fluidised bed furnaces. It is shown that the simple zirconia cell probe can be used to estimate the local air ratio of the gas above the bottom bed region of a fluidised bed furnace under the condition that the furnace is not operated under extreme oxidising or reducing conditions. The analysis of the signal from the zirconia cell is simplified by considering the time fractions of oxidising and reducing conditions, from which the local air ratio of the gas is estimated in any position in the furnace where fluctuations occur. This requires the determination of two parameters (σ and μ) of a given function, relating the time under oxidising conditions measured by the zirconia cell sensor and the local air ratio measured by gas analysis (Eq. (5)). The parameters depend on the fuel properties and on the position in the furnace. The method could be used as a cheap and simple arrangement to monitor the local air ratios at various heights, for example when utilising staged over-fire air in order to minimise emission of nitrous oxides.

The measurements also give information about the frequency of fluctuations between reducing and oxidising gas conditions, which is valuable for various combustion studies. An example of such studies is modelling of sulphur capture by limestone [7].

Detection of bubbles in a fluidised bed combustor by zirconia cell sensors is difficult because the oxidising fraction

of the gas depends not only on the bubble properties, but also on the overall air to fuel ratio and on the fuel properties. Furthermore, small oxidising regions cannot be detected since the response time of the sensor limits its resolution.

References

[1] K. Bergqvist, Zirconia cell measurements of fluctuations between oxidizing and reducing conditions in a circulating fluidized bed boiler, Licentiate Thesis, in Energy Conversion, Chalmers University of Technology, Göteborg, 1995.

[2] M.A. Rocazella, I.G. Wright, J. Campbell, Characterization and comparison of corrosive environments in fluidized bed coal combustors, Mater. Perform. 24 (5) (1985) 39–44.

[3] J.F. Stubington, S.W. Chan, The interpretation of oxygen-probe measurements in fluidized-bed combustors, J. Inst. Energy 63 (456) (1990) 136–142.

[4] P.M. Walsh, C. Li, A. Dutta, J.M. Beer, An interpretation of time-resolved oxygen concentration measurements in coal-burning fluidized beds, Inst. Chem. Eng. Symp. Ser. Chem. React. Eng. 87 (1984) 53–60.

[5] J. Stenberg, L.E. Åmand, R. Hernberg, B. Leckner, Measurements of gas concentrations in a fluidized bed combustor using laser-induced photoacoustic spectroscopy and zirconia cell probes, Combust. Flame 113 (4) (1998) 477–486.

[6] D.P. Saari, R.J. Davini, Evaluation of instruments for in-bed oxygen measurements in a fluidized-bed combustor, in: Proceedings of the International Conference on Fluidized Bed Combustion, vol. 7, No. 2, 1983, pp. 995–1009.

[7] A. Lyngfelt, K. Bergqvist, F. Johnsson, L.-E. Åmand, B. Leckner, Dependence of sulfur capture performance on air staging in a 12 MW circulating fluidized bed boiler, in: R. Clift, J.P.K. Seville (Eds.), Gas Cleaning at High Temperatures, Blackie, Glasgow, 1993, pp. 470–491.

[8] M.J. Fernandez, A. Lyngfelt, F. Johnsson, Gas concentrations in the lower part of the combustion chamber of a circulating fluidized bed boiler: influence of bed height, Energy Fuels 14 (6) (2000) 1127–1132.

[9] A.D. Brailsford, M. Yussouff, E.M. Logothetis, A first-principles model of the zirconia oxygen sensor, Sens. Actuators B 44 (1–3) (1997) 321–326.

[10] H. Rau, W. Schwartz, Problems of the gas potentiometric measurement of redox equilibria in flames, Chemische Technik (Leipzig, Germany) 37 (4) (1985) 169–172.

[11] A.D. Brailsford, E.M. Logothetis, Selected aspects of gas sensing, Sens. Actuators B 52 (1–2) (1998) 195–203.

[12] A.J. Minchener, J. Stringer, The use of electrochemical probes for measuring oxygen partial pressures within a fluidized-bed, J. Inst. Energy 57 (430) (1984) 240–251.

[13] E.B. Ljungström, In-bed oxygen measurements in a commercial-size AFBC, in: Proceedings of the International Conference on Fluidized Bed Combustion, vol. 8, No. 2, 1985, pp. 853–64.

[14] M.J. Fernandez, A. Lyngfelt, B.M. Steenari, Reaction between limestone and SO_2 under conditions alternating between oxidizing and reducing. The effect of short cycle times, Energy Fuels 14 (3) (2000) 654–662.

[15] P.F.B. Hansen, K.D. Johansen, K. Oestergaard, High-temperature reaction between sulfur dioxide and limestone. V. The effect of periodically changing oxidizing and reducing conditions, Chem. Eng. Sci. 48 (7) (1993) 1325–1341.

[16] V. Wiesendorf, E.-U. Hartge, J. Werther, F. Johnsson, J. Sterneus, B. Leckner, D. Montat, P. Briand, The CFB boiler in Gardanne—an experimental investigation of its bottom zone, in: Proceedings of the International Conference on Fluidized Bed Combustion, vol. 15, 1999, pp. 1514–1524.

[17] C.F. Holt, A.A. Boiarski, H.E. Carlton, The gas turbine heat exchanger in the fluidized bed combustor, in: Proceedings of the International Conference on Fluidized Bed Combustion, vol. 7, No. 1, 1983, pp. 295–305.

[18] B. Leckner, M.R. Golriz, W. Zhang, B.A. Andersson, F. Johnsson, Boundary layers—first measurements in the 12 MW CFB research plant at Chalmers University, in: Proceedings of the 11th International Conference on Fluidized Bed Combustion, 1991, pp. 771–776.